



## Photolysis and TiO<sub>2</sub> photocatalysis of the pharmaceutical propranolol: Solar and artificial light

N. De la Cruz, R.F. Dantas, J. Giménez\*, S. Esplugas

Department of Chemical Engineering, Faculty of Chemistry, University of Barcelona, C/Martí i Franquès, 1. 08028 Barcelona, Spain

### ARTICLE INFO

#### Article history:

Received 4 July 2012

Received in revised form

28 September 2012

Accepted 2 October 2012

Available online 11 October 2012

#### Keywords:

Emerging contaminants

Propranolol

Advanced oxidation process

Direct photolysis

Photocatalysis

TiO<sub>2</sub>

Solar

Xe-lamp

### ABSTRACT

This study focuses on the removal of the pharmaceutical propranolol (PRO) by direct photolysis and TiO<sub>2</sub> photocatalysis. Two different devices were employed, one at laboratory scale with artificial light (Xe-lamp) and the other one at pilot scale using solar irradiation. The solar plant was based on CPCs photoreactors. Solar radiation was quantified by a radiometer. To compare both devices, radiation was also measured using actinometrics. PRO degradation and mineralization were assessed to establish the feasibility of both treatments.

For direct photolysis, the influence of wavelength ranges was evaluated. In addition, reactors made with different materials (quartz and Duran) were also tested. Significant PRO degradation could be observed employing quartz reactors in both devices. PRO removal achieved after 240 min was 77% and 71% for the solar and the laboratory device, respectively. However, mineralization accomplished resulted to be negligible (7% and 2%).

For photocatalysis, different TiO<sub>2</sub> concentrations (0.1, 0.2, 0.4 g L<sup>-1</sup>) were tested. When 0.4 g L<sup>-1</sup> was used, the best results could be observed in both installations. PRO degradation percentages achieved after 240 min were 81% at the solar plant and 94% at laboratory. Meanwhile, mineralization reached was 30% and 41% in solar plant and laboratory device respectively.

In order to compare the different catalyst loads at the two devices, kinetics were evaluated as a function of time and energy involved. As TiO<sub>2</sub> concentration increased, higher reaction rates were obtained in both devices. In general, the laboratory device gave rates 1.1–1.5 times higher than the solar installation.

Biodegradability (BOD<sub>5</sub>/COD), oxidation (COD) and toxicity (algae *Chlorella vulgaris*) evolution during solar photocatalysis were followed. Biodegradability improved slightly from 0 to 0.06 after 270 min for the solar device, remaining non-biodegradable. Toxicity, measured in percentage of photosynthesis inhibition, decreased with treatment time. Oxidation of intermediates was observed, as COD underwent a reduction of 30% after 270 min.

This article also provides a section comparing different techniques found in literature employed for PRO abatement.

© 2012 Elsevier B.V. All rights reserved.

## 1. Introduction

Occurrence, impact and removal, from waters, of pharmaceuticals, considered as emerging contaminants (ECs), has been the target of many studies in the last decades [1–7].

Pharmaceuticals found in wastewaters come from hospitals, pharmaceutical industry or domestic wastewater as rejected drugs not used or from human excretions, as they are partially metabolized by human bodies [4]. The particularity of these chemicals is that conventional sewage treatment plants (STP) are not able to completely degrade them. Thus, pharmaceuticals fate ends up

being surface or sea waters, where they can cause adverse effects due to their biological potency toward flora, fauna, and humans [8–11].

Among pharmaceuticals, we found propranolol (PRO). It is a sympatholytic non-selective beta blocker. Sympatholytics are used to treat hypertension, anxiety and panic. It was the first successful beta blocker developed. This drug has been reported to be found in the aquatic environment, including waste water [12–17]. Its removal in STP is recognized to be less than 20%. Moreover, adsorption is the dominant mechanism of removal for this compound instead of biodegradation [8]. Several studies have also informed about the potential toxic effects of this pharmaceutical [4,18–20].

Advanced oxidation processes (AOPs) constitute a promising technology for the treatment of wastewaters containing pharmaceuticals [21,22]. These techniques are based on the generation of

\* Corresponding author. Tel.: +34 934021293; fax: +34 934021291.

E-mail address: [j.gimenez.fa@ub.edu](mailto:j.gimenez.fa@ub.edu) (J. Giménez).

hydroxyl radicals, the second highest known oxidant species. Thus, these processes are able to oxidize and mineralize almost every organic compound.

Among AOPs, photocatalysis has shown a great potential as a low-cost, environmental friendly and sustainable treatment technology. As known, heterogeneous photocatalysis is a process based on the interaction of light and a semiconductor. The semiconductor  $\text{TiO}_2$  has been widely utilized as catalyst. When a photon with energy equal to higher than  $\text{TiO}_2$  bandgap (3.2 eV for anatase and 3.0 eV for rutile) arrives to the catalyst surface an electron is photo-excited from the valence to the conduction band. The wavelength range with energy higher than  $\text{TiO}_2$  band gap is  $\lambda < 390 \text{ nm}$ . This mechanism generates electron-hole pairs which lead to a chain of redox reactions related to organic contaminants degradation [23].

PRO photocatalytic studies have been reported [24–26], but none of them have employed natural solar light before. The artificial generation of photons is the most important source of costs during photocatalysis. The use of sunlight would represent then a more economic and ecologic alternative. With a typical UV-flux of  $20\text{--}30 \text{ W m}^{-2}$ , near the surface of the Earth, the sun provides  $0.2\text{--}0.3 \text{ mol photons m}^{-2} \text{ h}^{-1}$  in the  $300\text{--}400 \text{ nm}$  range, available for the catalyst activation. Photoreactor selection is also an important key point for solar photocatalytic processes. For solar photochemical applications, compound parabolic concentrators (CPCs) constitute a good option. They are static and collect direct and diffuse solar radiation. They are able to concentrate on the receiver all the radiation that arrives within the angle of acceptance of collectors. The normal values for the semi-angle of acceptance ( $\theta_a$ ), for photocatalytic applications, are between  $60$  and  $90^\circ$ . When this angle is  $90^\circ$  (non-concentrating solar system), the concentrating factor is equal to one ( $R_C = 1$ ). In this case, all the UV radiation that reaches the aperture area of the CPC (direct and diffuse) can be collected and redirected to the tubular reactor [27,28].

The aim of this work was to evaluate PRO degradation by direct photolysis and  $\text{TiO}_2$  photocatalysis by using two different devices, with artificial (Xe-lamp) and natural solar light. Compound degradation, mineralization, biodegradability and acute toxicity were the selected parameters to study the feasibility of the process. Another aim was to study the kinetics of degradation, based on time and energy involved. Results obtained can be useful to establish comparisons between laboratory and solar devices. This study also summarizes information found in literature about PRO abatement by different techniques (direct photolysis and AOPs).

## 2. Materials and methods

### 2.1. Chemicals

Aqueous pharmaceutical solutions were prepared in Milli Q water with PRO [318-98-9], which was purchased from Sigma-Aldrich Chemical Co (Fig. 1). Synthetic amorphous titanium dioxide (Degussa P-25) was used as received. Fig. 1 shows the structure of the target pharmaceutical.

For actinometries o-nitrobenzaldehyde (98%) and ethanol (96% v/v), from Panreac Química, were employed.

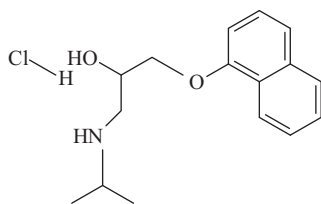


Fig. 1. PRO (β-blocker) molecular structure.

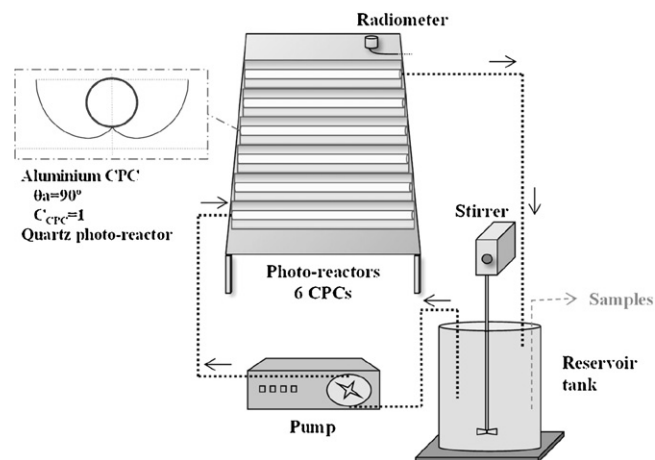


Fig. 2. Solar pilot plant. Barcelona  $41^\circ 28' \text{N}$ ,  $2^\circ 06' \text{E}$ , sea level.

### 2.2. Analytical procedures

PRO concentrations were monitored by a high-performance liquid chromatograph (HPLC) from Waters using a SEA18 5 μm  $15 \times 0.46$  Teknokroma column, and a Waters 996 photodiode array detector. Data were analyzed with the Empower Pro software 2002 Water Co. The mobile phase was composed by water (pH 3) and acetonitrile (70:30) injected with a flow rate of  $0.80 \text{ mL min}^{-1}$ . PRO samples injection volume was  $10 \text{ μm}$ . Detection was done at maximum UV absorbance set at wavelength of  $213.7 \text{ nm}$ . In order to remove the catalyst, before the HPLC analysis, samples were filtered with a polyethersulfone membrane filter of  $0.45 \text{ μm}$ .

Total organic carbon (TOC) was measured in a Shimadzu TOC-V CNS instrument. PRO absorption spectrum was determined with a PerkinElmer UV/VIS Lambda 20 (200–700 nm range) spectrophotometer.

Biochemical oxygen demand ( $\text{BOD}_5$ ) determinations were carried out according to the Standard Methods (5120) by the OxiTop® procedure.

To analyze the chemical oxygen demand (COD), the Standard Methods (5220D) procedures were followed.

For the toxicity assessment, the LuminoTox® analysis was used. The LuminoTox® SAPS test kit consists on a fluorometer biosensor that uses stabilized aqueous photosynthetic systems (SAPS) to recognize toxic chemicals in water by measuring photosynthetic activity. SAPS are algae (*Chlorella vulgaris*) that fluoresce when photosynthesis is activated by light absorption.  $100 \text{ μL}$  of SAPS solution are spiked on  $2 \text{ mL}$  of sample. The endpoint is established at  $15 \text{ min}$  represented by  $IC_{50}$  (Inhibitory concentration causing 50% light loss) expressed in %.

### 2.3. Experimental devices

#### 2.3.1. Solar device

Solar photocatalytic experiments were carried out in a pilot plant located in Barcelona (latitude  $41^\circ 28' \text{N}$ , longitude  $2^\circ 06' \text{E}$ , at sea level, September–November 2011). The photoreactor consisted in a module of 6 parallel CPCs (concentration factor of 1,  $C_{\text{CPC}} = 1$ ) made of polished aluminum, with a total mirror's area of solar irradiation caption-reflection of  $0.228 \text{ m}^2$ , tubular quartz receivers and  $41^\circ$  inclined (Fig. 2). The irradiated volume was  $0.95 \text{ L}$ . There was a mechanical stirred reservoir tank of  $10 \text{ L}$ . The solution with the pharmaceutical and  $\text{TiO}_2$  in suspension was continuously recirculated employing a pump (peristaltic pump Ecoline VC-380, ISMATEC) through the photoreactors and the reservoir tank. Temperature was not controlled and it could vary from  $20$  to  $30^\circ \text{C}$ .

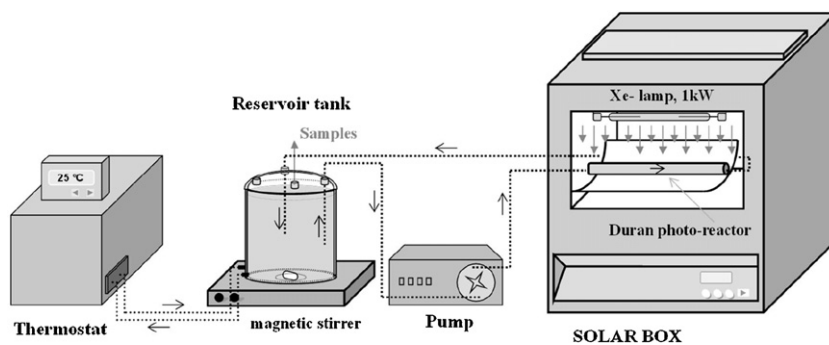


Fig. 3. Laboratory installation. Xe-lamp.

### 2.3.2. Laboratory device

A stirred reservoir tank (1.0 L) was filled with the pharmaceutical-TiO<sub>2</sub> (suspended) aqueous solution. The aqueous suspension was continuously pumped (peristaltic pump Ecoline VC-280) into the Solarbox (Co. fo.me.gra 220V, 50 Hz) and recirculated to the reservoir tank (Fig. 3). In the Solarbox, the Duran tubular photoreactor (0.078 L) was irradiated by a Xe-OP lamp (Phillips 1 kW). The photoreactor was placed at the bottom of the Solarbox in the axis of a parabolic mirror. When necessary, a filter (cut-off <280 nm) located just below the lamp, was used. In order to keep the solution at 25 °C, the jacket temperature of the stirred tank was controlled with an ultra-thermostat bath (Haake K10). All connections and pipes employed were made of Teflon and/or glass material to avoid losses by adsorption.

Table 1 shows the main characteristics of both devices.

### 2.4. Radiation measurements

Radiation was measured in two different ways: with an actinometer and a radiometer.

Actinometry(o-nitrobenzaldehyde, 290–400 nm [29,30]) was carried out at the two devices: solar and Xe-lamp. Thus, results could be compared in both installations by using the same method for radiation measurement. The initial solution was prepared with o-NB 2.5 × 10<sup>-3</sup> mol L<sup>-1</sup> using water/ethanol 50:50 as solvent. The solution was treated in both installations as they worked for the photocatalytic experiments. Samples were collected from the reservoir tank every 5 min after irradiation started, from time zero (before irradiating). Samples were analyzed on HPLC (SEA18 5 μm 15 × 0.46 Teknokroma column, mobile phase water/acetonitrile (40:60) 0.6 mL min<sup>-1</sup>, injection volume 5 μL, detected at 258 nm), in order to follow the o-NB concentration during the procedure and calculate the photonic flow [30].

Table 1  
Experimental devices.

Plant	Solar pilot plant	Laboratory plant
Reactor's material	Quartz	Duran
Radiation	Solar light	Xe-OP lamp (Phillips 1 kW)
Total volume (L)	10 L	1 L
Volume irradiated/Total volume (%)	9.5	8.4
Total length irradiated (cm)	395	24.0
Internal diameter (cm)	1.75	2.11
Thickness (cm)	0.15	0.20
Pump flow rate (mL min <sup>-1</sup> )	2609	714
Initial pharmaceutical concentration	50 mg L <sup>-1</sup>	50 mg L <sup>-1</sup>

During solar experiments, irradiance was always followed using a radiometer (Delta OHM, LP 471 UVA). It was placed on the CPCs platform with the same orientation and inclination. It provided data in terms of direct irradiation (315–400 nm) in W m<sup>-2</sup> (UV<sub>G</sub>). Thus, results could be referred to accumulated energy, Q<sub>UV,n</sub> (kJ L<sup>-1</sup>), calculated by Eq. (1) [31].

$$Q_{UV,n} = Q_{UV,n-1} + \Delta t_n \overline{UV}_{G,n} \frac{A_{CPC}}{V_{TOT}} \quad (1)$$

( $\Delta t_n = t_n - t_{n-1}$ )

where  $t_n$  is the experimental time for each sample (s),  $\overline{UV}_{G,n}$  the average UV<sub>G</sub> during  $\Delta t_n$ ,  $A_{CPC}$  the collectors surface (0.228 m<sup>2</sup>) and  $V_{TOT}$  the total plant volume (10 L).

## 3. Results and discussion

### 3.1. Direct photolysis of propranolol. Artificial and solar light

Propranolol direct photolysis experiments were conducted at laboratory scale under artificial irradiation (Xe-lamp) and in a pilot plant under solar light. Employing the Xe-lamp, almost all experiments were conducted using a filter cutting off wavelengths shorter than 280 nm, in order to approximate to solar irradiation. Experiments were done in duplicate with an average standard deviation of 0.022 ± 0.019. All experiments were performed starting with 50 mg L<sup>-1</sup> of PRO.

At laboratory scale, two different photo-reactors were employed, one made of quartz and the other one made of Duran. When experiments were performed using the filter ( $\lambda < 280$  nm), both photo-reactors gave similar behavior on the degradation evolution (Fig. 4). After 240 min, percentages of degradation achieved were 37.9 and 28.8% for quartz and duran, respectively. Meanwhile, mineralization observed was insignificant, obtaining 8.7 and 4.2% after the same time.

Duran is known to cut off irradiation with wavelengths under ~300 nm. Meanwhile quartz allows the pass of radiation with wavelengths higher than 200 nm. Since Xe-lamp starts irradiating around 230 nm, the experiment using the quartz photo-reactor was also developed without the filter. Thus, PRO photolytic impact was observed when part of the UV-C range was involved. In this case, transformation resulted to be much more significant. PRO removal achieved was 71.4% after 240 min and 84% after 360 min. However, mineralization accomplished resulted to be negligible (1.9%, at 240 min) the same as when the filter was present.

At the solar pilot plant, where photo-reactor tubes were made of quartz, a removal of 77.3% was achieved after 240 min (Barcelona, September 2011). Mineralization accomplished after the same time was 6.6%.

Very similar percentages of degradation were observed using solar or artificial light with quartz reactors (without filter), when

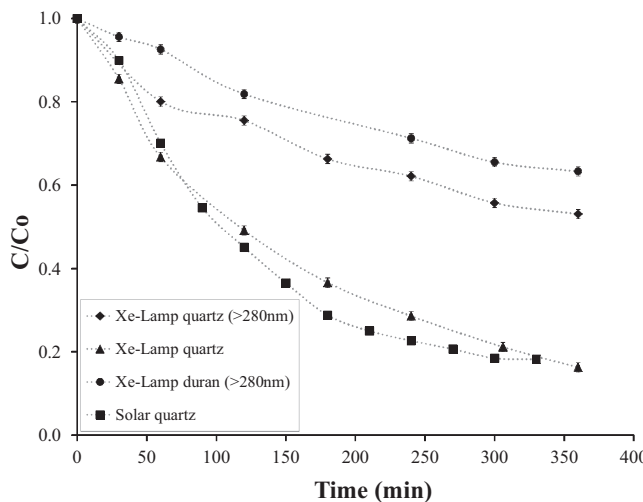


**Fig. 4.** Photolytic treatment of PRO (initial concentration  $50 \text{ mg L}^{-1}$ ). Normalized PRO concentration (with standard deviation) versus time.

degradation was represented versus time. Even if degradation profiles were similar in these two cases, other parameter must be taken into account for better comparison. This is the accumulated energy. In this way, actinometries (*o*-nitrobenzaldehyde, 290–400 nm [29,30]) were carried out at the two devices to know the involved average photonic flow. From these experiences, total accumulated energy at the solar plant resulted to be 30 kJ (after 240 min), meanwhile at the laboratory device it was 13 kJ (after 240 min). It could be seen that much more accumulated energy was needed at the solar plant to achieve similar degradation. This could be explained because, with Xe-lamp, PRO was also being photolyzed by irradiation at the more energetic range of UV-C, which is negligible in solar irradiation.

PRO absorbing spectra is also presented to better understand the photolysis. This compound has main UV absorption peaks centered around 214 and 290 nm (Fig. 5). With quartz photo-reactors, light with wavelengths lower than 300 nm could be absorbed by PRO. It can also be observed that, with Xe-lamps and quartz reactors, there is a wavelength range (230–240 nm) where PRO absorbs significantly. This was supported by the high percentage of removal observed in this case, where an 84% was degraded after 360 min.

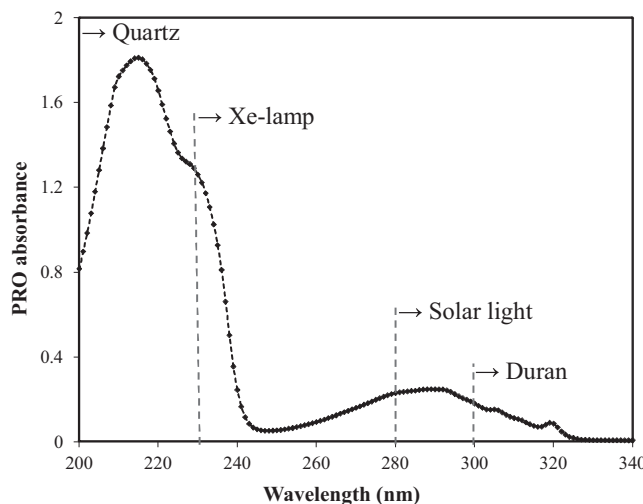


**Fig. 5.** PRO absorbance at different wavelengths. Cut-off wavelengths for quartz and Duran and active wavelengths for Xe-lamp and sun-light.

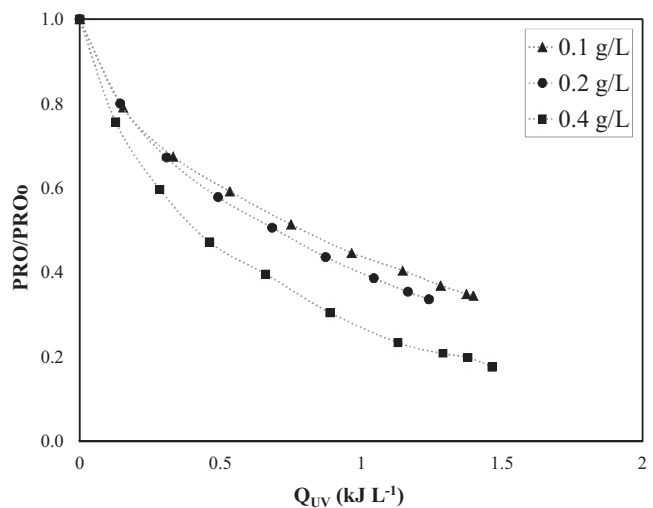


**Fig. 6.** Solar pilot device. Photocatalytic treatment of PRO (initial concentration  $50 \text{ mg L}^{-1}$ ) at different catalyst loads. Normalized PRO concentration versus accumulated energy (measured by radiometer, Eq. (1)).

Summarizing, PRO degradation shown in experiments of Fig. 4 is due to direct photolysis, since there are no other photosensitive compounds in water which could be able to generate reactive species, such as hydroxyl radicals. In addition, this fact can explain the negligible mineralization observed if it is compared with photocatalytic experiments (Section 3.2.1.3).

### 3.2. Photocatalysis of propranolol.

Photocatalytic treatments using  $\text{TiO}_2$  in suspension were performed to know its influence on PRO degradation. The same devices used in photolytic experiments were employed: solar light at pilot scale (10 L) and Xe-lamp at laboratory (1 L). Experiments were done at least in duplicate. Main goals chased in this case were the comparison of these two light sources, the observation of degradation profiles as well as the mineralization, oxidation, kinetics, biodegradability and toxicity evolution.

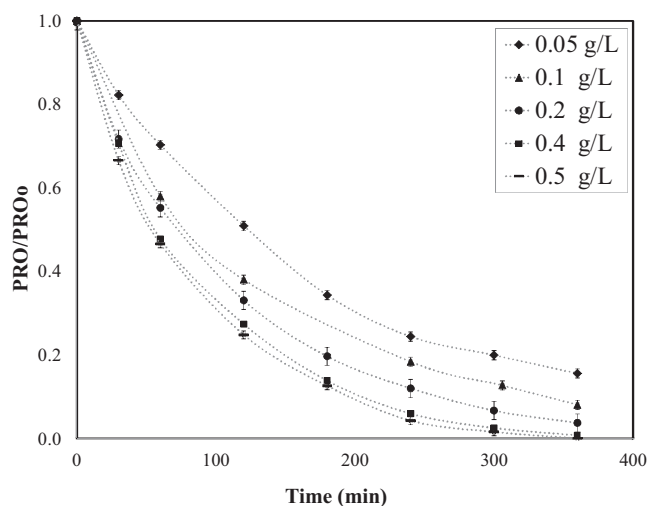


**Fig. 7.** Xe-lamp, laboratory device. Photocatalytic treatment of PRO (initial concentration  $50 \text{ mg L}^{-1}$ ) at different catalyst loads. Normalized PRO concentration (with standard deviation) versus time.

**Table 2**Pseudo-first order kinetic constants ( $k_{ap}$ ) for  $C=f(t)$  (180 min) for solar and artificial light.  $r^2$ : coefficient of determination.

Device	$TiO_2$ (g L <sup>-1</sup> )	$k_{ap}$ (min <sup>-1</sup> )	$r^2$	Device	$TiO_2$ (g L <sup>-1</sup> )	$k_{ap}$ (min <sup>-1</sup> )	$r^2$
Solar plant	0.1	0.00492	0.9865	Xe-lamp	0.1	0.00901	0.9989
Solar plant	0.2	0.00518	0.9909	Xe-lamp	0.2	0.00925	0.9956
Solar plant	0.4	0.00785	0.9975	Xe-lamp	0.4	0.01085	0.9983

**Table 3**Pseudo-first order kinetic constants ( $k'_{ap}$ ) for  $C=f(Q_{UV})$  (after 9 kJ, o-nitrobenzaldehydeactinometry).  $r^2$ : coefficient of determination.

Device	$TiO_2$ (g L <sup>-1</sup> )	$k'_{ap}$ (kJ <sup>-1</sup> )	$r^2$	Device	$TiO_2$ (g L <sup>-1</sup> )	$k'_{ap}$ (kJ <sup>-1</sup> )	$r^2$
Solar plant	0.1	0.1039	0.9865	Xe-lamp	0.1	0.1756	0.9970
Solar plant	0.2	0.1121	0.9909	Xe-lamp	0.2	0.1773	0.9956
Solar plant	0.4	0.1620	0.9975	Xe-lamp	0.4	0.2079	0.9983

### 3.2.1. Solar and artificial light. Influence of catalyst load

**3.2.1.1. Degradation.** Three different catalyst loads were used, 0.1, 0.2 and 0.4 g L<sup>-1</sup> for the different irradiation sources tested, solar light and Xe-lamp (with a filter cutting off wavelengths under 280 nm). In both cases, as the catalyst load increased in this range, the degradation observed was also higher.

Degradation percentages achieved, after 240 min at the solar plant for 0.1, 0.2 and 0.4 g L<sup>-1</sup>, were 64.8% (November 2011,  $Q_{UV}$ : 1.4 kJ L<sup>-1</sup>), 65.4% (November 2011,  $Q_{UV}$ : 1.2 kJ L<sup>-1</sup>), 80.5% (October 2011,  $Q_{UV}$ : 1.4 kJ L<sup>-1</sup>) (Eq. (1)), respectively (Fig. 6). Percentages of removal, at laboratory device with Xe-lamp after 240 min, were 81.6, 88.0, 94.1% for the three different  $TiO_2$  concentrations (Fig. 7). This entails 1.2–1.4 times higher degradations at the laboratory device. For the best condition (laboratory device and 0.4 g L<sup>-1</sup> of catalyst) 360 min were needed for total PRO removal (99%).

With the laboratory device, another concentration was also tested, 0.5 g L<sup>-1</sup>, to observe when  $TiO_2$  saturation occurs. In this case, PRO degradation evolution was quite similar to that obtained for 0.4 g L<sup>-1</sup> (Fig. 7). After 240 min, degradation reached was 95.7% and PRO was not detected after 360 min. Higher catalyst concentrations were not employed to avoid depositions inside the system.  $TiO_2$  load of 0.05 g L<sup>-1</sup> was also tested to widen the response for low concentrations. After 240 min degradation was 75.6%.

**3.2.1.2. Kinetics.** In the photocatalytic experiments, PRO concentration evolution ( $C$ ) was fitted to pseudo-first order kinetics. In this

treatment, the main reaction for PRO removal was the one between the compound and hydroxyl radicals. To simplify, as  $^{\bullet}OH$  species have very short lives, in this equation the kinetic constant ( $k_{ap}$ ) has this term implicit (Eq. (2)).

$$r = k_{OH}[^{\bullet}OH]C = k_{ap}C \quad (2)$$

Kinetics were fitted as a function of time ( $C=f(t)$ ) for the two experimental devices. Furthermore, to better compare, they were also calculated as a function of accumulated energy ( $C=f(Q_{UV})$ ). Following this purpose, actinometry (o-nitrobenzaldehyde, 290–400 nm) was performed to estimate the average photonic flow involved in both cases.  $K_{ap}$  values could be respectively obtained from the slopes of the regression curves representing  $-\ln(C/C_0)$  vs time or accumulated energy (for the same accumulated energy at both devices of 9 kJ). Obtained results are summarized in Tables 2 and 3.

As  $TiO_2$  concentration increased, higher kinetic constants were obtained in both devices. Fastest rates of degradation were observed for the laboratory device, being the higher one for the biggest amount of  $TiO_2$ , 0.4 g L<sup>-1</sup>. In general, this device gave constant rates 1.3–1.8 higher than the solar installation.

**3.2.1.3. Mineralization, oxidation, biodegradability and toxicity.** Mineralization was also followed for all the experiments at different catalyst loads and the two experimental devices tested.

Mineralization achieved after 240 min at the solar plant, for 0.1, 0.2 and 0.4 g L<sup>-1</sup>, was 11.3, 15.8 and 30.4% (same experimental

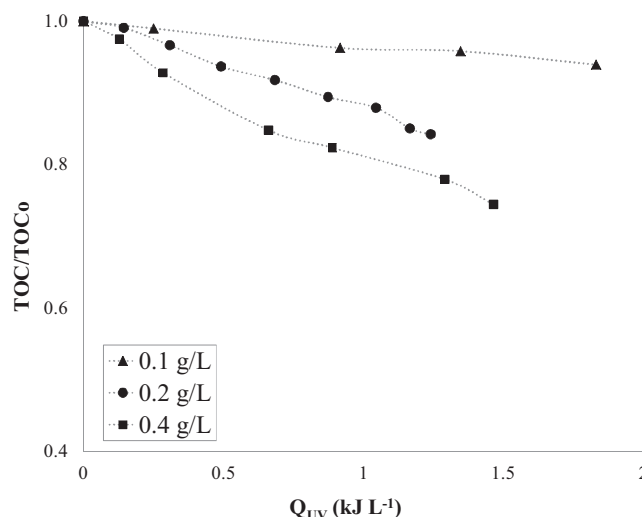


**Fig. 8.** Solar light pilot device. Mineralization of PRO (initial concentration 50 mg L<sup>-1</sup>) for different catalyst loads. Normalized TOC concentration versus accumulated energy (measured by radiometer, Eq. (1)).

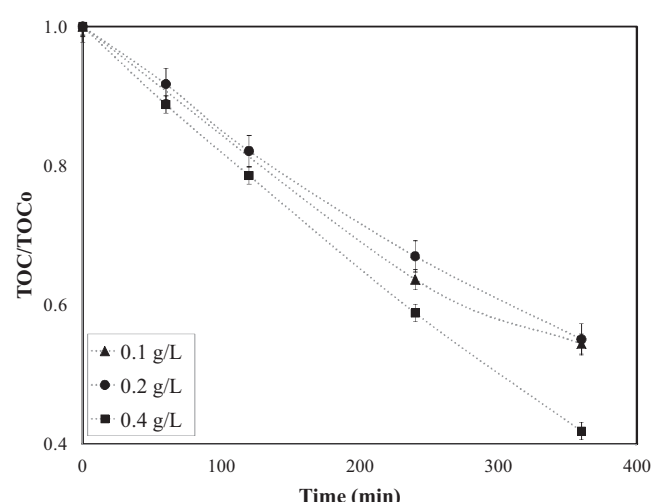


**Fig. 9.** Xe-lamp, laboratory device. Mineralization of PRO (initial concentration 50 mg L<sup>-1</sup>) for different catalyst loads. Normalized TOC (with standard deviation) versus time.

**Table 4**

Treatments of pharmaceutical propranolol in waters by direct photolysis (D.P.) and AOPs.

Technique	Matrix/Initial PRO concentration	Conditions	Results	Ref.
D.P.	Milli-Q water-air/50 mg L <sup>-1</sup>	Xe-lamp 1 kW, reactors: <sup>1</sup> Duran, <sup>2</sup> quartz, <sup>3</sup> quartz (>280 nm). Sun light (41 °N) (Sep'11), <sup>4</sup> quartz reactor	$k_p^1: 0.117 \text{ h}^{-1}$ , $k_p^2: 0.338 \text{ h}^{-1}$ , $k_p^3: 0.129 \text{ h}^{-1}$ $k_p^4: 0.427 \text{ h}^{-1}$	P.S.
D.P.	Milli-Q water-air/1–2 µg L <sup>-1</sup>	Xe-lamp 1.1 kW (290–700 nm), quartz reactor, $T^a$ 20 °C, pH 7	$k_p: 0.16 \text{ h}^{-1}$ , $t_{1/2}: 4.4 \text{ h}$ , $\varphi: 0.0260$	[32]
D.P.	Deionizedwater/1 mg L <sup>-1</sup>	Xe-lamp 1.1 kW (290–800 nm), quartz reactor, $T^a$ 20 °C	$k_p: 0.033 \text{ h}^{-1}$ , $t_{1/2}: 21 \text{ h}$	[33]
D.P.	Pure water/10 µg L <sup>-1</sup> and 10 mg L <sup>-1</sup>	HP Mercury lamp 125 W (280–600 nm), Pyrex reactor	$t_{1/2}: 8 \text{ h}$ (10 µg L <sup>-1</sup> ), 8 h (10 mg L <sup>-1</sup> )	[34]
D.P.	Purewater/100 µg L <sup>-1</sup>	Sun light (34 °N) ( <sup>1</sup> Aug'06, <sup>2</sup> May'07), quartz reactor	$k_p^1: 0.12 \text{ h}^{-1}$ , $t_{1/2}^1: 6.0 \text{ h}$ , $\varphi^1: 0.017$ $k_p^2: 0.084 \text{ h}^{-1}$ , $t_{1/2}^2: 8.3 \text{ h}$ , $\varphi^2: 0.019$	[35]
D.P.	Purewater/5–137 µg L <sup>-1</sup>	LP Mercury lamps <sup>1</sup> (254 nm) and <sup>2</sup> (254+185 nm), quartz	$k_p^1: 4.6 \cdot 10^{-4} \text{ s}^{-1}$ , $k_p^2: 2.5 \cdot 10^{-3} \text{ s}^{-1}$	[36]
D.P.	Deionizedwater/50 mg L <sup>-1</sup>	Mercury lamp 30 W (254 nm), direct radiation, free pH	$k_p: 0.04 \text{ h}^{-1}$ , $\varphi: 0.07$	[37]
Photocatalysis	Milli-Q/50 mg L <sup>-1</sup>	Xe-lamp 1 kW - Duran reactor <sup>1</sup> Sun light (41 °N) (October–November 11) – quartz reactor <sup>2</sup> (TiO <sub>2</sub> P25-suspension), $T^a < 30 \text{ }^\circ\text{C}$ , neutral pH, $t: 180 \text{ min}$	$k_{ap}^1: 0.00901$ , $0.0185 \text{ min}^{-1}$ (0.1, 0.4 g L <sup>-1</sup> TiO <sub>2</sub> ) $k_{ap}^2: 0.00492$ , $0.00785 \text{ min}^{-1}$ (0.1, 0.4 g L <sup>-1</sup> TiO <sub>2</sub> )	P.S.
Photocatalysis	Milli-Q/50 mg L <sup>-1</sup>	Xe-lamp 1 kW – Duran reactor (0.4 g L <sup>-1</sup> TiO <sub>2</sub> P25-suspension), $T^a$ 25 °C, neutral pH	remotion at 360 min $k_{ap}: 0.0118 \text{ min}^{-1}$ (300 min)	[25]
Photocatalysis	Milli-Q/100 µM <sup>1</sup> , 200 µM <sup>2</sup>	HP Mercury lamp 125 W, Pyrex reactor, $2 \text{ g L}^{-1}$ (TiO <sub>2</sub> P25-suspension), pH 7	$k_{ap}^1: 0.182 \text{ min}^{-1}$ , 100% removal (40 min) $k_{ap}^2: 0.078 \text{ min}^{-1}$	[26]
Photocatalysis	Milli-Q/5 mg L <sup>-11</sup> , 20 mg L <sup>-12</sup>	Xe-lamp 1 kW, 0.25 g L <sup>-1</sup> (TiO <sub>2</sub> P25-suspension), $T^a < 30 \text{ }^\circ\text{C}$ , neutral pH	% removal (120 min): 78% <sup>1</sup> , 40% <sup>2</sup>	[24]
Ozonation	Effluent WWTP + Reverse osmosis/1.05 µg L <sup>-1</sup>	5 mg L <sup>-1</sup> O <sub>3</sub> , $T^a$ 20–22 °C, pH 7	$k_{O3}: 1 \times 10^5 \text{ M}^{-1} \text{ s}^{-1}$ , removal in 0.8 s	[38]
Ozonation	Effluent WWTP (after 2 <sup>IV</sup> clarifier)/36 ng/L	0.36 Nm <sup>3</sup> /h O <sub>3</sub> , $T^a$ 25 °C, pH 7.63	ozone dose for remotion: <50 µM	[39]
Ozonation	Milli-Q/0.38 mmol/L	0.34 g/h O <sub>3</sub> , $T^a$ 24 °C	remotion at <4 min remotion at 8 min (0.47 mmol/L O <sub>3</sub> ) (pH 4)	[40]
UV/H <sub>2</sub> O <sub>2</sub>	<sup>1</sup> Pure water, <sup>2</sup> Biologically treated WW /119 µg L <sup>-1</sup>	LP Mercury lamps 8 W (254 nm), $T^a$ 20 °C, pH 7	$k_{ap}^1: 3.1 \cdot 10^{-3} \text{ s}^{-1}$ , $k_{ap}^2: 1.7 \cdot 10^{-3} \text{ s}^{-1}$	[41]
Fenton	Effluent WWTP/1 µg L <sup>-1</sup>	H <sub>2</sub> O <sub>2</sub> :Fe(II) = 2.5 (molar), $T^a$ amb, pH 3, $t: 30 \text{ min}$	Fe(II) dose to: 50% removal (2.5 mg L <sup>-1</sup> ), 90% removal (8.2 mg L <sup>-1</sup> )	[42]

<sup>1</sup> $k_p$ : first order kinetic constant, <sup>2</sup> $k_{ap}$ : apparent first order kinetic constant,  $k_{O3}$ : second order kinetic constant, P.S.: present study.

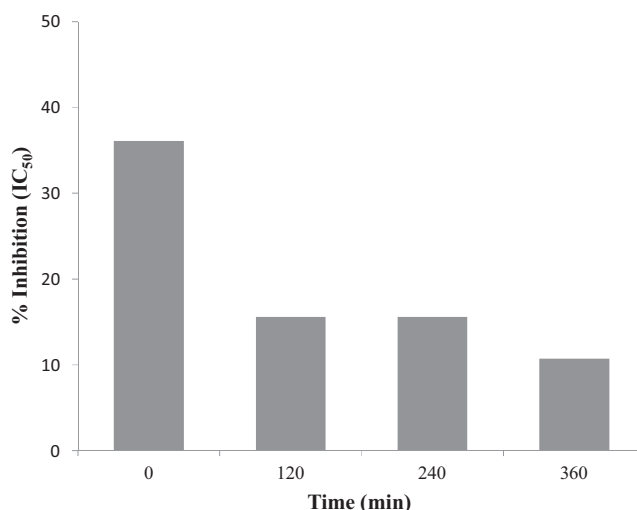


**Fig. 10.** Toxicity Luminotox®. Solar photocatalysis ( $0.4 \text{ g L}^{-1}$   $\text{TiO}_2$ ,  $50 \text{ mg L}^{-1}$  PRO).

conditions as in Section 3.2.1.1), respectively (Fig. 8). Percentages of mineralization, at the laboratory plant with the Xe-lamp after 240 min, were 36.6, 33.0 and 41.1% for the three different  $\text{TiO}_2$  concentrations (Fig. 9). In this case, the laboratory device was also more effective in terms of time, having percentages of mineralization 1.4–3.2 times higher than these ones obtained at the solar device. Attending to the catalyst concentrations, best results were achieved for the highest  $\text{TiO}_2$  concentration tested,  $0.4 \text{ g L}^{-1}$ . In this way, the best global mineralization was achieved at the laboratory plant with  $0.4 \text{ g L}^{-1}$  of  $\text{TiO}_2$ . For these conditions, after 360 min, when almost no PRO could be found (99% of degradation), mineralization reached was 58.1%.

Laboratory device gave also best results for oxidation evolution. Experiments were developed for  $50 \text{ mg L}^{-1}$  of PRO and  $0.4 \text{ g L}^{-1}$  of  $\text{TiO}_2$ . Measuring COD, this parameter underwent a reduction of 29.6% for the solar device after 270 min, and 51.8% for the laboratory device.

Biodegradability ( $\text{BOD}_5/\text{COD}$ ) at the solar device was also monitored. This is an important parameter in case this process would come before a biological treatment. Experiments were performed for the same conditions of PRO and catalyst. An initial solution of  $50 \text{ mg L}^{-1}$  of PRO gave almost zero for this biodegradability indicator. After being treated for 270 min at the solar device (31% of PRO degradation), biodegradability improved slightly until 0.06 for this indicator. This means the solution remains being considered not biodegradable. In previous work, at the laboratory device, almost no improvement on the biodegradability could be observed at least until 250 min of photocatalysis. However, after 360 min of treatment, at the point of almost complete PRO degradation (~99%), biodegradability indicator reached 0.7, higher than 0.4, that indicates it could be considered biodegradable [25].

Toxicity evolution was also tested for the photocatalytic solar experiment, employing  $0.4 \text{ g L}^{-1}$  of  $\text{TiO}_2$ . Initial PRO concentration was  $50 \text{ mg L}^{-1}$ . Tests were performed with Luminotox®. The toxic potential caused by the presence of PRO in water and its transformation by solar photocatalysis process was observed. Analyses were made from the initial untreated solution until 360 min every 120 min. Results are shown in Fig. 10.

Toxicity, measured in percentage of inhibition, decreased with prolonging treatment time. In the first two hours this percentage dropped from 36% until 16%. Then, stabilization could be seen, followed by other decreasing until 11% after 360 min. The Luminotox® assay suggested that transformation induced by the solar photocatalytic process promoted the formation of less toxic compounds.

This corroborates the suitability of this technique for PRO degradation.

### 3.3. Comparison of different PRO removal studies in literature

In this section different PRO removal studies found in literature are presented (Table 4). Techniques selected were direct photolysis and AOPs such as photocatalysis, ozonation,  $\text{UV}/\text{H}_2\text{O}_2$  and Fenton. In Table 4, main operating conditions and results in terms of removals and kinetics are summarized.

Attending to direct photolysis employing Xe-lamps, first order kinetic constants ( $k_p$ ) observed were in the same order of magnitude, for very different initial concentrations. Thus, for initial concentrations of  $1\text{--}2 \mu\text{g L}^{-1}$ ,  $1 \text{ mg L}^{-1}$  and  $50 \text{ mg L}^{-1}$ ,  $k_p$  were  $0.16$ ,  $0.033$  and  $0.129 \text{ h}^{-1}$ , respectively [32,33]. Kinetics were found less similar for solar experiments, with values for  $k_p$  of  $0.427 \text{ h}^{-1}$  (present study) and  $0.12 \text{ h}^{-1}$  [35].

Most efficient AOP for PRO removal was found to be ozonation, very low reaction times were needed for total abatement (0.8 s, 4 min and 8 min) [38,39,21].  $\text{UV}/\text{H}_2\text{O}_2$  was also a fast technique, with a half-life of 3.73 min (calculated from the kinetic constant as  $\ln(2)/k_{ap}$ ) for  $119 \mu\text{g L}^{-1}$  of PRO [40]. Fenton could degrade 50% of  $1 \mu\text{g L}^{-1}$  of PRO in 30 min with  $2.5 \text{ mg L}^{-1}$  of Fe (II) [41]. Photocatalytic experiments, with  $50 \text{ mg L}^{-1}$  of PRO,  $0.4 \text{ g L}^{-1}$  of  $\text{TiO}_2$  and Xe-lamp, needed 60 min to degrade 50%, and 90 min when solar light was employed. It must be said that photocatalytic experiments here summarized used high initial concentrations in comparison with other AOPs presented, so times for removal must also be much higher.

## 4. Conclusions

Solar photocatalysis at pilot scale has been demonstrated to be useful on the removal of PRO from waters (81% of degradation was reached, 240 min). Important mineralization (30%) could be also observed during the treatment.

This process was also developed using a Xe-lamp at laboratory scale (94% of degradation and 41% of mineralization) and compared.

Similar results for different catalyst loads were observed for the two devices. Percentage of degradation improved with higher  $\text{TiO}_2$  concentrations. Comparing PRO degradation rates in function of the energy involved (measured by actinometry), the laboratory device resulted to be 1.3–1.7 times faster.

Solar photocatalysis could improve toxicity of waters containing PRO. Slight increase on biodegradability could be observed with this method on the period of time tested.

Direct photolysis contributed significantly to PRO transformation with both light sources and when reactors were made of quartz: 71% in the laboratory device and 77% in the solar plant (240 min). However, this technique provided poor index of mineralization: 2% in the laboratory device and 7% in the solar plant.

## Acknowledgements

Authors are grateful to CICYT Projects CTQ2008-01710 and CTQ2011-26258, Consolider-Ingenio NOVEDAR 2010 CSD2007-00055 and AGAUR-Generalitat de Catalunya (project 2009SGR 1466) for funds received to carry out this work. Authors are also grateful to Spanish ministry of economy and competitiveness (FPI research fellowship, ref. BES-2009-022963).

## References

- [1] N. De la Cruz, J. Giménez, S. Esplugas, D. Grandjean, L.F. De Alencastro, C. Pulgarín, Water Research 46 (2012) 1947–1957.
- [2] S.D. Richardson, T.A. Ternes, Analytical Chemistry 83 (2011) 4616–4648.

- [3] I. Oller, S. Malato, J.A. Sánchez-Pérez, *Science of The Total Environment* 409 (2011) 4141–4166.
- [4] L.H.M.L.M. Santos, A.N. Araújo, A. Fachini, A. Pena, C. Delerue-Matos, M.C.B.S.M. Montenegro, *Journal of Hazardous Materials* 175 (2010) 45–95.
- [5] S. Vilhunen, M. Sillanpää, *Reviews in Environmental Science and Biotechnology* 9 (2010) 323–330.
- [6] S. Esplugas, D.M. Bila, L.G.T. Krause, M. Dezotti, *Journal of Hazardous Materials* 149 (2007) 631–642.
- [7] M. Petrović, S. Gonzalez, D. Barceló, *TrAC Trends in Analytical Chemistry* 22 (2003) 685–696.
- [8] D. Fatta-Kassinos, S. Meric, A. Nikolaou, *Analytical and Bioanalytical Chemistry* 399 (2011) 251–275.
- [9] C.M. Coetsier, S. Spinelli, L. Lin, B. Roig, E. Touraud, *Environment International* 35 (2009) 787–792.
- [10] N. Bolong, A.F. Ismail, M.R. Salim, T. Matsuura, *Desalination* 238 (2009) 229–246.
- [11] M. Maurer, B.I. Escher, P. Richle, C. Schaffner, A.C. Alder, *Water Research* 41 (2007) 1614–1622.
- [12] J. Martín, D. Camacho-Muñoz, J.L. Santos, I. Aparicio, E. Alonso, *Journal of Environmental Monitoring* 13 (2011) 2042–2049.
- [13] D. Camacho-Muñoz, J. Martín, J.L. Santos, I. Aparicio, E. Alonso, *Journal of Hazardous Materials* 183 (2010) 602–608.
- [14] C. Fernández, M. González-Doncel, J. Pro, G. Carbonell, J.V. Tarazona, *Science of The Total Environment* 408 (2010) 543–551.
- [15] V. Gabet-Giraud, C. Miège, J.M. Choubert, S.M. Ruel, M. Coquery, *Science of The Total Environment* 408 (2010) 4257–4269.
- [16] A. Ginebreda, I. Muñoz, M.L. de Alda, R. Brix, J. López-Doval, D. Barceló, *Environment International* 36 (2010) 153–162.
- [17] A. Pal, K.Y.H. Gin, A.Y. Lin, M. Reinhard, *Science of The Total Environment* 408 (2010) 6062–6069.
- [18] S. Franzellitti, S. Buratti, P. Valbonesi, A. Capuzzo, E. Fabbri, *Aquatic Toxicology* 101 (2011) 299–308.
- [19] H. Ericson, G. Thorsén, L. Kumblad, *Aquatic Toxicology* 99 (2010) 223–231.
- [20] K. Fent, A.A. Weston, D. Caminada, *Aquatic Toxicology* 76 (2006) 122–159.
- [21] R.F. Dantas, C. Sans, S. Esplugas, *Journal of Environmental Engineering* 137 (2011) 754–759.
- [22] M. Klavarioti, D. Mantzavinos, D. Kassinos, *Environment International* 35 (2009) 402–417.
- [23] M.N. Chong, B. Jin, C.W.K. Chow, C. Saint, *Water Research* 44 (2010) 2997–3027.
- [24] L.A. Ioannou, E. Hapeshi, M.I. Vasquez, D. Mantzavinos, D. Fatta-Kassinos, *Solar Energy* 85 (2011) 1915–1926.
- [25] V. Romero, N. De La Cruz, R.F. Dantas, P. Marco, J. Giménez, S. Esplugas, *Catalysis Today* 161 (2011) 115–120.
- [26] H. Yang, T. An, G. Li, W. Song, W.J. Cooper, H. Luo, X. Guo, *Journal of Hazardous Materials* 179 (2010) 834–839.
- [27] S. Malato, P. Fernández-Ibáñez, M.I. Maldonado, J. Blanco, W. Gernjak, *Catalysis Today* 147 (2009) 1–59.
- [28] S.M. Rodríguez, J.B. Gálvez, M.I.M. Rubio, P.F. Ibáñez, D.A. Padilla, M.C. Pereira, J.F. Mendes, J.C. De Oliveira, *Solar Energy* 77 (2004) 513–524.
- [29] J.M. Allen, S.K. Allen, S.W. Baertschi, *Journal of Pharmaceutical and Biomedical Analysis* 24 (2000) 167–178.
- [30] K.L. Willett, R.A. Hites, *Journal of Chemical Education* 77 (2000) 900–902.
- [31] S. Malato, J. Blanco, C. Richter, B. Milow, M.I. Maldonado, *Chemosphere* 38 (1999) 1145–1156.
- [32] A.Y-C. Lin, M. Reinhard, *Environmental Toxicology and Chemistry* 24 (2005) 1303–1309.
- [33] Q.-T. Liu, H.E. Williams, *Environmental Science and Technology* 41 (2007) 803–810.
- [34] A. Piram, A. Salvador, C. Verne, B. Herbreteau, R. Faure, *Chemosphere* 73 (2008) 1265–1271.
- [35] H. Yamamoto, Y. Nakamura, S. Moriguchi, Y. Nakamura, Y. Honda, I. Tamura, Y. Hirata, A. Hayashi, J. Sekizawa, *Water Research* 43 (2009) 351–362.
- [36] I. Kim, H. Tanaka, *Environment International* 35 (2009) 793–802.
- [37] R.F. Dantas, O. Rossiter, A.K.R. Teixeira, A.S.M. Simões, V.L. da Silva, *Chemical Engineering Journal* 158 (2010) 143–147.
- [38] J. Benner, E. Salhi, T. Ternes, U. vonGunten, *Water Research* 42 (2008) 3003–3012.
- [39] R. Rosal, A. Rodríguez, J.A. Perdigón-Melón, A. Petre, E. García-Calvo, M.J. Gómez, A. Agüera, A.R. Fernández-Alba, *Water Research* 44 (2010) 578–588.
- [40] I. Kim, N. Yamashita, H. Tanaka, *Chemosphere* 77 (2009) 518–525.
- [41] W. Li, V. Nanaboina, Q. Zhou, G.V. Korshin, *Water Research* 46 (2012) 403–412.